Metabolomics Identifies and Validates Serum Novel Biomarker for Diagnosing Primary Angle Closure Glaucoma and Predicting the Visual Field Progression

Shengjie Li[1,2,3,4,5#*], Jun Ren[1#], Yichao Qiu[1], Zhendong Jiang [1], Mingxi Shao[1], Yingzhu Li[1], Jianing Wu[1], Yunxiao Song[6], Xinghuai Sun[2,3,4,5], Wenjun Cao[1,2,3,4,5*]

1. Department of Clinical Laboratory, Eye & ENT Hospital, Shanghai Medical College, Fudan University, Shanghai, China

2. Department of Ophthalmology & Visual Science, Eye & ENT Hospital, Shanghai Medical College, Fudan University, Shanghai, China

3. State Key Laboratory of Medical Neurobiology, Institutes of Brain Science, Fudan University, Shanghai, China

4. Key Laboratory of Myopia, Chinese Academy of Medical Sciences, Shanghai, China

5. NHC Key Laboratory of Myopia, Fudan University, Shanghai, China

6. Department of Clinical Laboratory, Shanghai Xuhui Central Hospital, Fudan University, Shanghai, China

* These authors contributed equally.

Corresponding author:

Shengjie Li, Eye & ENT Hospital, Shanghai Medical College, Fudan University, Fenyang Road 83th, Shanghai 200031, China. E-mail: lishengjie6363020@163.com

Wenjun Cao, Eye & ENT Hospital, Shanghai Medical College, Fudan University, Fenyang Road 83th, Shanghai 200031, China. E-mail: wgkjyk@aliyun.com

Running head: Androstenedione as a diagnostic and predictive biomarker for PACG

Figures: 7

Tables: 2

Supplementary Tables: 10

Supplementary Figures: 14

Abstract

Background: Primary angle closure glaucoma (PACG) is the leading cause of irreversible blindness worldwide, and no reliable, effective diagnostic, and predictive biomarkers are used in clinical routines. A growing body of evidence shows metabolic alterations in patients with glaucoma. we aimed to develop and validate potential metabolite biomarkers to diagnose and predict the visual field progression of PACG.

Methods: Here, we used a 5-phases (discovery phase, validation phase 1, validation phase 2, supplementary phase, and cohort phase) multicenter (EENT hospital, Shanghai Xuhui central hospital), cross-sectional, prospective cohort study design to perform widely-targeted metabolomics and chemiluminescence immunoassay to determine candidate biomarkers. Five machine learning (random forest, support vector machine, lasso, K-Nearest neighbor, and Gaussian NB) approaches were used to identify an optimal algorithm. The discrimination ability was evaluated using the area under the receiver operating characteristic curve (AUC). Calibration was assessed by Hosmer-Lemeshow tests and calibration plots.

Results: Studied serum samples were collected from 616 participants, and 1464 metabolites were identified. Machine learning algorithm determines that androstenedione exhibited excellent discrimination and acceptable calibration in discriminating PACG across the discovery phase (discovery set 1, areas under the receiver operating characteristic curve [AUC] =1.0 [95%CI, 1.00-1.00]; discovery set, AUC=0.85 [95%CI, 0.80-0.90]) and validation phases (internal validation, AUC=0.86 [95%CI, 0.81-0.91]; external validation, AUC=0.87 [95%CI, 0.80-0.95]). Androstenedione also exhibited a higher AUC (0.92-0.98) to discriminate the severity of PACG. In the supplemental phase, serum androstenedione levels were consistent with those in aqueous humor (r=0.82, P=0.038) and significantly (P=0.021) decreased after treatment. Further, cohort phase demonstrates that higher baseline androstenedione levels (hazard ratio=2.71 [95% CI: 1.199-6.104], P=0.017) were associated with faster visual field progression.

Conclusion: Our study demonstrates serum androstenedione as a novel biomarker that can be used to diagnose PACG and predict visual field progression.

Keywords: primary angle closure glaucoma; metabolomics; androstenedione; diagnose; predict; visual field progression; biomarker

1. Background

Glaucoma is the most frequent cause of irreversible blindness worldwide[1], and its prevalence is increasing globally, making it a public health concern[2]. Primary angle-closure glaucoma (PACG) is a major form of glaucoma in east Asian ethnic patients, affecting 70% of glaucoma patients worldwide[3–5]. Hence, early detection of PACG and accurate prediction of visual field (VF) changes can potentially preserve vision and mitigate the risk of PACG advancement. Measurement of intraocular pressure, perimetry, gonioscopy and optical coherence tomography is the main diagnostic testing to assess for glaucoma and to monitor for disease progression[6]. However, the present clinical techniques are inadequate for the early diagnosis and prognosis of VF progression as they depend on specialized eye examination equipment and the expertise of ophthalmologists. Furthermore, patients seldom seek the services of an ophthalmologist until the symptoms worsen or visual acuity significantly deteriorates. Importantly, the He et al.[7] taught us that performing laser iridotomy on patients with 180 degrees of angle closure does not prevent PACG, thus gonioscopy may not a good tool to help distinguish PACG from controls. Therefore, the development of a straightforward and dependable biomarker or biomarker panel to facilitate early detection and prognostication of progressive visual field loss in primary angle-closure glaucoma is imperative, rather than relying solely on the expertise of ophthalmologists and specialized equipment.

Multiple etiology and risk factors lead to the onset/development of PACG in humans, which involves a tremendous flow of physiological changes, genetic factors, and metabolic adaptations[8]. Both physiological changes, genetic factors, and metabolic adaptations should lead to profound changes in most metabolic pathways. Small molecule metabolites, as crucial biomarkers of cellular function[9], which identifies and quantified by metabolomics, are the omics product closest to clinical phenotypes[10]. A burgeoning corpus of evidence indicates metabolic changes in individuals afflicted with glaucoma[11–15]. Nevertheless, extant metabolomics research on glaucoma is constrained by inadequate sample sizes, a dearth of validation sets to corroborate findings, and an absence of specificity analyses. Notably, investigations have yet to comprehensively characterize the serum metabolome in sizable cohorts to identify putative biomarkers capable of distinguishing patients with PACG from healthy controls.

In this study, a cross-sectional and prospective cohort design was employed to systematically profile blood metabolites using widely-targeted metabolomics and chemiluminescence immunoassay in both

patients with primary angle-closure glaucoma (PACG) and normal subjects. The objectives of the study were to characterize the metabolic profile associated with PACG, identify potential blood diagnostic biomarkers of PACG, assess the specificity of diagnostic biomarkers for PACG of any severity, and verify the biomarkers used to predict the visual field progression of PACG.

2. Methods

2.1 Participant

From January 2020 to December 2021, newly diagnosed PACG and age-sex-matched normal controls were recruited from the Eye Center of Fudan University and Shanghai Xuhui Central hospital. Detailed ophthalmic examinations and medical examinations were described in the supplementary material. Approval from the Institutional Review Board/Ethics Committee (2020[2020013]) was obtained from the Ethics Committee of the Eye and ENT Hospital, and the study adhered to the principles of the Declaration of Helsinki. Informed consent was obtained from all subjects.

A glaucoma specialist diagnosed PACG. The diagnostic criteria for PACG were described previously[16–18] and detailed in the supplementary material. The inclusion and exclusion criteria of patients with PACG were described previously[16–18] and detailed in the supplementary material. The methods performed for VF analysis were done as previously described[16,18] and detailed in the supplementary material. Previously described methods[16,18–20] were performed for the determination of functional PACG VF loss progression according to an event-based analysis modified for Octopus perimetry.

2.2 Study design

A cross-sectional, multicenter, prospective cohort study design. In the cross-sectional study, a total of 616 patients and normal controls were prospectively enrolled from the Eye Center of Fudan University and Shanghai Xuhui Central hospital which was divided into 4 phases (discovery phase [discovery set 1, the discovery set 2], validation phase 1 [external validation], validation phase 2 [internal validation], supplemental phase) from eight districts in China (Figure S1). The 5 phases of the study are independent and are shown in Figure 1. The discovery set 1 was composed of 80 serum samples from PACG patients and 60 samples from normal controls which was enrolled from Eye Center of Fudan University between January 2020 to June 2020. The discovery set 2 was composed of 100 serum

samples from PACG patients and 80 samples from normal controls which was enrolled from Eye Center of Fudan University between July 2020 to Deccember 2020. The differential metabolites of discovery set 1 and discovery set 2 were obtained by widely-targeted metabolomics. The intersection of the differential metabolites of the two discovery sets was used as a candidate biomarker. For validation phase 1, serum samples from 70 PACG patients and 50 normal controls were collected which was enrolled from Shanghai Xuhui Central hospital between January 2020 to December 2020. Candidate biomarkers were validated in validation phase 1 using widely-targeted metabolomics, and potential biomarkers were obtained. For validation phase 2, serum samples from 98 PACG patients and 78 normal controls were collected which was enrolled from Eye Center of Fudan University between January 2021 to December 2021. Potential biomarkers were validated in validation phase 2 using chemiluminescence methods. For the supplemental phase, we used widely-targeted metabolomics to investigate whether the same potential biomarkers were present in PACG patients' aqueous humor. All the clinical characteristics (Age, sex, BMI, hypercholesterolemia, hypertension, diabetes, smoking, drinking) were matched between PACG and normal controls in the 4 phases.

In the prospective cohort study, 98 newly diagnosed PACG patients were included from the Eye Center of Fudan University between January 2020 and December 2020. All participants visited once every six months to allow regular assessment of PACG disease progression (the minimum follow-up period was set to 24 months). Serum samples from 98 PACG patients were collected and measured using chemiluminescence methods. Detailed information of patients follow up were described as previously[16,18].

2.3 Sample preparation

2.3.1 Sample collection

The blood was collected prior to the treatment. Briefly, subjects were asked to ensure about eight-ten hours of fasting before sampling. Venous blood samples were collected in heparinized tubes between 7:00-9:30 am. The clinical laboratory obtained the sample at about 10:00 am and centrifuged them at 3000rpm for 10min. Then serum was collected into a sterilized cryotube and immediately stored at -80°C for metabolomic analysis.

The acquisition of aqueous humor was described previously[13]. Aqueous humor (AH) was collected by skilled ophthalmologists during the surgical treatment of PACG and cataract patients. AH was obtained

at the start of the procedure using a fine-bore needle during a corneal paracentesis. Following that, AH samples were quickly transferred to sterile cryotubes and kept at -80 °C for metabolomic analysis.

2.3.2 Sample preprocessing

Before extraction, the serum was thawed on ice, vortex for 10s and mixed well. 300μL of pure methanol was added to 50μL of serum, swirled for 3min, and centrifuged at 12000 rpm for 10min at 4°C. After centrifugation, transfer the supernatant into a new centrifuge tube and place it in a -20°C refrigerator for 30 minutes. The sample was thawed on ice and centrifuged at 12000r/min for 3 minutes—Transfer 180μL of the supernatant to the injection vial for mass spectrometry analysis. Quality control (QC) samples are generated by pooling all the serum samples to monitor the retention time and signal intensity consistency. Equal volumes (10 μL) of all serum samples were combined to generate quality control (QC) samples, which were employed to monitor the repeatability of the analysis. During the mass spectrometry analysis, one QC sample was included in every ten samples to ensure the consistency of the analytical process. The PACG and control groups' serum samples were randomly arranged and analyzed. The laboratory conducting the metabolomics measurements was blinded to the samples' case/control/QC status.

2.4 Detection method[21]

2.4.1 Untargeted detection conditions

Ultra Performance Liquid Chromatography (UPLC) (ExionLC AD, AB SCIEX) separation was performed using Waters ACQUITY HSS T3 (2.1×100mm, 1.8um). The oven temperature was set to 40°C, and the sample injection volume was 5 μL. Metabolites were eluted from the column at a flow rate of 0.35 mL/min. Mobile phases for UPLC consisted of 0.1% acetic acid in water (phase A) and 0.1% acetic acid in acetonitrile (phase B). The following gradient elution program was employed: 0-10min: linear gradient from 5% to 90% B; 10-11min: 90% B; 11-11.1min: linear gradient from 90% to 5% B; 11.1-14min: 5% B. Metabolic extracts were analyzed by the triple time of flight (TOF) mass spectrometer (TripleTOF 6600, AB SCIEX) in both positive and negative ionization modes. The scan range was 50-1,000 m/z. Electrospray ionization (ESI) source conditions were set as follows: ion spray voltage (IS) 5500V (positive), -4500V (negative); ion source gas I (GSI), gas II (GASII), curtain gas (CUR) was set at 50,50, and 25 psi, respectively; collision energy (CE) 30V.

2.4.2 Widely targeted detection conditions

UPLC (ExionLC AD, AB SCIEX) separation was performed using Waters ACQUITY UPLC C18(2.1×100mm, 1.8um). The oven temperature was set to 40℃, and the sample injection volume was 2 μL. Metabolites were eluted from the column at a flow rate of 0.35 mL/min. Mobile phases for UPLC consisted of 0.1% acetic acid in water (phase A) and 0.1% acetic acid in acetonitrile (phase B). The following gradient elution program was employed: 0-11min: linear gradient from 5% to 90% B; 11-12min: 90% B; 12-12.1min: linear gradient from 90% to 5% B; 12.1-14min: 5% B. Metabolic extracts were analyzed by the triple quadrupole-linear ion trap mass spectrometer (QTRAP 6500, AB SCIEX) in both positive and negative ionization modes. ESI source conditions were set as follows: ion spray voltage (IS) 5500V (positive), -4500V (negative); ion source gas I (GSI), gas II (GASII), curtain gas (CUR) was set at 50,50, and 25 psi, respectively. Each ion pair is scanned for detection based on optimized voltage and CE.

2.4.3 Metabolite profiling

Mixed samples were made and tested by AB Triple TOF 6600 mass spectrometer. The detected metabolites were identified based on Metware in-house database, Metware public database (Metlin, HMDB, KEGG), and MetDNA. Score the identified metabolites, and screen the metabolites with a total score > 0.5. MRM was used for the mixed samples to determine the final ion pair and other information. Based on the new database (metabolites with a total score > 0.5 + Metware in-house database), Q-trap 6500 was used to quantify all samples accurately. The workflow of mass spectrometry is detailed in Figure S2.

2.4.4 Data processing

All LC-MS data were processed using Analyst 1.6.3 for imputing raw, peak picking, alignment, and normalization to produce peak intensities for retention time and m/z data pages. The features were selected based on their CV with QC samples. Features with CVs of more than 15% were eliminated.

2.4.5 Chemiluminescence immunoassay

Serum levels of androstenedione were measured using a commercially available kit (Snibe Diagnostics, Shenzhen, China) and were determined using the chemiluminescent immunoassay method by Roche Cobase e 601 (Germany).

2.5 Sample size and missing value

In the cross-sectional study, to calculate the minimum total sample size, we used an open-source

calculator based on the methods described by Obuchowski et al.[22] and Li et al.[23]. The input parameters were specificity = 0.9 (allowable error = 0.05), sensitivity = 0.9 (allowable error = 0.05), α = 0.05 (2-tailed). Based on this calculation, the minimum sample size required for the new biomarker was 98 per phase.

An unreliable conclusion would result from missing data, which would introduce bias. Thus no patients with missing data were included in this study. In this study, a total of 48 participants (lack of VF value = 18, lack of medication history record = 12, lack of intraocular pressure [IOP] value = 10, loss to follow-up = 8) were excluded due to with missing data.

2.6 Statistical analysis

Normality was assessed using the Shapiro–Wilk W-test. Independent student's t-test, Kruskal-Wallis test, one-way ANOVA, Wilcox test, and chi-square tests were used when appropriate. Results are presented as frequency and percentage for categorical variables, mean ± SD for normally distributed continuous variables, and median (interquartile range) for not normally distributed continuous variables. The Spearman correlation test was used to determine the significance of the correlations between the variables.

Diagnostic efficiency was evaluated using receiver operating characteristic (ROC) curves. Five machine learning (random forest, support vector machine, lasso, K-nearest neighbor [KNN], and Gaussian Naive Bayes [NB]) approaches were used to identify an optimal algorithm. The Youden index maximizing sensitivity plus specificity is applied to determine the best cutoff value, sensitivity, specificity, accuracy, positive predictive value (PPV), and negative predictive value (NPV) were also calculated. Hosmer-Lemeshow tests were used to assess the goodness of fit. The calibration of the biomarker was assessed by computing the calibration plot. Hanley-McNeil method was used to compare these AUCs.

Unsupervised principal component analysis (PCA) was performed by statistics function prcomp withe R. The data was unit variance scaled before unsupervised PCA. Supervised orthogonal projections to latent structures-discriminate analysis (OPLS-DA) were applied to obtain a higher level of group separation and a better understanding of variables responsible for classification. Heatmaps of samples and metabolites were carried out by R package (ComplexHeatmap; heatmap). In order to evaluate the binding mode of metabolites and proteins, Autodock Vina v.1.2.2 was used to analyze molecular

docking. Fold change= the characteristic peak area of metabolites in the PACG group / the control group.

Identified metabolites were annotated using the KEGG Compound database (http://www.kegg.jp/kegg/ compound/). Then annotated metabolites were mapped to the KEGG Pathway database (http://www.kegg.jp/kegg/pathway.html). Significantly enriched pathways were identified with a hypergeometric test's p-value for metabolites.

Cox proportional hazards analysis was also carried out to investigate the relationship between baseline androstenedione levels and VF progression loss. The HRs and baseline characteristics that would assist in categorizing participants into the non-progressing PACG group over the follow-up period were determined using Cox proportional hazards models. Kaplan-Meier plots were used to study the survival results, and the log-rank test was applied to see whether there were any differences between the produced plots.

All statistical analyses were performed using R programming language and SPSS 13.0 (SPSS Inc., Chicago, IL, USA), a list of statistical approaches and packages detailed in table S1. P-values less than 5% were considered statistically significant.

Role of funding sources

The funder of the study had no role in study design, data collection, data analysis, data interpretation, or writing of the report.

3. Results

3.1 Metabolomic analyses in samples from PACG patients and normal controls

The design of this study is depicted in Figure 1, while the clinical features of all participants in the four phases of the study are presented in Tables 1 (Phases 1-3) and S2-S3 (Phase 4). All clinical characteristics, including age, sex, BMI, hypercholesterolemia, hypertension, diabetes, smoking, and drinking, were carefully matched between the PACG and normal control groups across all four phases. Following rigorous quality control, data filtering, and normalization procedures, a total of 1464 metabolites were identified across the various samples (N = 440). During the discovery phase, the OPLS-DA analysis revealed notable distinctions between participants with primary angle-closure glaucoma (PACG) and those without the condition (Figure 2A). Volcano plots (Figure 2B) were

generated using metabolites exhibiting a false discovery rate [FDR] of less than 0.1 and fold changes greater than 1.15 or less than 0.85. In discovery sets 1 and 2, 268 metabolites (21.5%) and 117 metabolites (9.6%), respectively, were found to be significantly altered between PACG and normal subjects.

The Venn diagram depicted in Figure 2C illustrates the presence of 32 metabolites that were found to be common in both discovery set 1 (as presented in table S4) and discovery set 2 (as presented in table S5). The parameters used for detecting these 32 differential metabolites are detailed in Table S6. Subsequently, these differential metabolites were utilized for conducting clustering analysis, which is visually represented in the form of a heatmap for both discovery set 1 (Figure 2D) and discovery set 2 (Figure 2E). These 32 differential metabolites were mainly related to alcohol and amines, amino acid and its metabolomics, benzene and substituted derivatives, fatty acid, heterocyclic compounds, hormones, and hormone-related compounds, nucleotide and its metabolomics, organic acid and its derivatives class (Figure 2D, 2E).

3.2 The blood differential metabolite discriminates PACG from normal

Can these metabolites in blood differentials be considered as potential biomarkers for PACG? In order to investigate this, we computed the area under the curve (AUC) for each of the 32 differential metabolites to evaluate their discriminatory capacity in distinguishing PACG from healthy individuals using five machine learning techniques (random forest, support vector machine, lasso, KNN, and Gaussian NB). Among these approaches, KNN demonstrated the highest performance in identifying PACG from normal controls. Subsequently, a 2-column heatmap was generated to display the resulting area under the curve (AUC) values for discovery set 1 and discovery set 2, respectively, as depicted in Figure 3A. The receiver operating characteristic (ROC) analysis of 32 metabolites revealed AUC values ranging from 0.74 to 1.0 in discovery set 1 and 0.72 to 1.0 in discovery set 2 for distinguishing PACG from normal subjects. The eigenmetabolite of the 32-metabolite cluster between PACG and normal subjects is illustrated in Figure 4B and 4C. The discriminatory accuracy of the metabolite in differentiating PACG from normal subjects using random forest, support vector machine, lasso, and Gaussian NB is presented in Figure S3.

The present study reveals that the eigenmetabolite levels were markedly elevated ($P<0.001$) in the normal group compared to the PACG group, as evidenced by the results obtained from discovery set

1 (Figure 3B) and discovery set 2 (Figure 3C). These findings provide compelling evidence that the heightened risk of PACG is linked to a robust blood metabolite signature.

3.3 Biomarker discovery to discriminates PACG from normal

Figure 3A illustrates that 32 metabolites were verified during the discovery phase and were subsequently identified as potential biomarkers. Figure 4A depicts a correlation analysis between ocular clinical characteristics and the 32 potential biomarkers discovered during the PACG discovery phase. Notably, a significant positive correlation was observed between androstenedione and the mean deviation of the VF (MD) ($r=0.45$, $P<0.001$). This correlation was also observed in discovery set 1 (Figure S4, $r=0.37$, $P<0.001$) and discovery set 2 (Figure S5, $r=0.50$, $P<0.001$), respectively. A statistically insignificant ($P>0.05$) correlation was observed between ocular clinical characteristics and the remaining 31 potential biomarkers, as depicted in Figure 3A, Figure S4, and Figure S5. Notably, the level of androstenedione was found to be significantly higher in PACG patients than in normal subjects in both discovery set 1 (Figure 4B, $P=0.0081$) and discovery set 2 (Figure 4C, $P=0.0078$). Additionally, high levels of androstenedione were identified as an independent risk factor for PACG, as shown in Table S7. Supplementary Figure 6 (Discovery set 1) and supplementary Figure 7 (Discovery set 2) illustrate the levels of the remaining 31 metabolites between PACG patients and normal subjects. Based on the preceding analysis, androstenedione was chosen using KNN due to its ability to differentiate between PACG and normal subjects. In discovery set 1, the AUC for PACG versus control was 1.0 (95% CI, 1.0 to 1.0), as shown in Figure 4D and Table S8. Similarly, in discovery set 2, PACG was identified with an AUC of 0.85 (95% CI, 0.80 to 0.90) when compared to control subjects, as depicted in Figure 4E and Table S8.

3.4 Biomarker validation in two independent validation phases

During the validation phases, Androstenedione was evaluated as a biomarker signature. The samples from validation phase 1 were subjected to LC-MS analysis for widely-targeted metabolomics, which revealed significant differences between PACG and normal participants, as demonstrated by the OPLS-DA analysis (Figure S8). In validation phase 2, a chemiluminescence immunoassay method was developed to enable precise quantification of serum androstenedione levels in a convenient and rapid manner.

During validation phase 1 and 2, the level of androstenedione was found to be significantly higher in

individuals with PACG compared to normal subjects (Figure 5A, P=0.0042; Figure 5B, P=0.0034). The performance of androstenedione was evaluated using the AUC in ROC analysis. The AUC for PACG versus control was 0.87 (95% CI, 0.80 to 0.95) in validation phase 1, as depicted in Figure 5C and Table S8. In validation phase 2, a consistent performance of androstenedione (AUC, 0.86, 95% CI, 0.81 to 0.91) was observed (Figure 5D, Table S8).

3.5 Biomarker validation in male and female subgroups

Validation of androstenedione as a biomarker for PACG necessitates consideration of sex, as males exhibit 5-10 times higher levels of this hormone than females. Accordingly, the subjects were stratified into male and female subgroups.

Figure S9 demonstrates that in the discovery phase, the AUC for PACG compared to control was 1.0 (95% CI, 1.0 to 1.0) in the male subgroup (Figure S9A), and 0.91 (95% CI, 0.85 to 0.98) in the female subgroup (Figure S9B). In validation phase 1, the AUC for PACG versus control was 0.83 (95% CI, 0.73 to 0.92) in the male subgroup (Figure S9C), and 1.0 (95% CI, 1.0 to 1.0) in the female subgroup (Figure S9D). In validation phase 2, the AUC for PACG versus control was 1.0 (95% CI, 1.0 to 1.0) in the male subgroup (Figure S9E), and 0.88 (95% CI, 0.79 to 0.98) in the female subgroup (Figure S9F).

3.6 Androstenedione associates with severity of PACG

The present study aimed to examine the potential association between serum androstenedione levels and the clinical severity of PACG. PACG severity was categorized into mild (MD≦6), moderate (6-12), and severe (MD >12) based on the MD value. The results from both discovery set 1 (Figure S10A) and discovery set 2 (Figure S10B) indicated that the mean serum androstenedione levels were significantly higher in the severe PACG group compared to the moderate and mild PACG groups (P<0.001). These findings were further validated in both validation phase 1 (Figure S10C) and validation phase 2 (Figure S10D).

A correlation analysis was conducted to examine the relationship between MD and androstenedione. Notably, a statistically significant positive correlation was found between MD and androstenedione in both discovery set 1 (Figure S4, r=0.37, P<0.001) and discovery set 2 (Figure S5, r=0.50, P<0.001). This finding was further confirmed in validation phase 2 (Figure S10E, r=0.61, P<0.001). Subsequently, the diagnostic potential of androstenedione in distinguishing the severity of PACG was investigated. An AUC was calculated for each severity of PACG to evaluate the discriminatory accuracy of

348 androstenedione in distinguishing between mild, moderate, and severe cases. The results of ROC
349 analysis indicated AUC values ranging from 0.75 to 0.95 in discovery set 1 (Figure S11A, Table S8)
350 and 0.94 to 0.99 in discovery set 2 (Figure S11B, Table S8) when using KNN machine learning
351 algorithms. The validity of androstenedione in distinguishing the severity of PACG was demonstrated
352 through consistent performance in both validation phase 1 (Figure S11C, Table S8, AUC of 0.64-0.97)
353 and validation phase 2 (Figure S11D, Table S8, AUC of 0.98-1.0). Additionally, when mild and
354 moderate cases were combined, the AUC for mild and moderate versus severe was 0.94 (95% CI 0.89
355 to 0.99) in discovery set 1 (Figure S10F, Table S8), 0.93 (95% CI 0.88 to 0.98) in discovery set 2
356 (Figure S10G, Table S8), 0.92 (95% CI 0.85 to 0.99) in validation phase 1 (Figure S10H, Table S8),
357 and 0.98 (95% CI 0.96 to 1.0) in validation phase 2 (Figure S10I, Table S8).

358 **3.7 Clinical value of androstenedione in patients with PACG**

359 The lack of specificity of serum biomarkers remains a significant obstacle to the clinical application
360 of such markers. To investigate temporal changes in androstenedione levels during the initial diagnosis
361 and post-treatment period, we conducted a random analysis of nine pairs of blood samples from
362 patients with primary angle-closure glaucoma (PACG) taken before and three months after therapy.
363 Our findings indicate a significant decrease in androstenedione levels in the post-treatment serum of
364 the 97th patient compared to the pre-treatment serum ($P = 0.021$). These findings showed that the levels
365 of androstenedione that were tightly connected with PACG severity rose dramatically as PACG
366 progressed.

367 A case-control study (PACG=7, Cataract=11) (Figure 6C) was conducted to investigate the potential
368 elevation of aqueous humor levels of androstenedione in patients with PACG. The findings revealed a
369 statistically significant increase ($P=0.011$) in the levels of androstenedione in the aqueous humor of
370 patients with PACG compared to those with cataracts (Figure 6D). Additionally, a significantly positive
371 correlation between MD and aqueous humor levels of androstenedione was observed (Figure 6E,
372 $r=0.98$, $P<0.001$). The mean aqueous humor levels of androstenedione were found to be significantly
373 higher ($P<0.001$) in the severe PACG group compared to the moderate and mild PACG groups (Figure
374 6F). Subsequently, an examination was conducted on seven paired serum-aqueous humor samples
375 obtained from identical PACG patients to ascertain the presence of a consistent pattern within the same
376 individuals. A statistically significant correlation was observed between the levels of androstenedione

in serum and aqueous humor (r=0.82, P=0.038) (Figure 6G).

3.8 Calibration ability of androstenedione on discovery phase and validation phase

Figure S12 displays the calibration plots for both the discovery and validation phases, which effectively validate the calibration performance of serum androstenedione for probability. The plots demonstrate a high level of agreement between predicted and observed values in both discovery set 1 (Figure S12A) and discovery set 2 (Figure S12B). The Hosmer-Lemeshow test yielded a nonsignificant statistic in the discovery set 1 (χ^2=0, P=1) and discovery set 2 (χ^2=6.16, P=0.10), indicating no departure from a perfect fit. Validation phase 1 (Figure S12C, χ^2=5.14, P=0.14) and validation phase 2 (Figure S12D, χ^2=1.25, P=0.26) resulted in similar performance.

3.9 Androstenedione could predict VF progression in patients with PACG

This study comprised 97 participants diagnosed with PACG, selected based on the screening criteria and followed up for a period of 24 months. In cases of bilateral PACG, one eye was selected at random. Of the total participants, 44 (45.36%) exhibited glaucoma progression, as evidenced by visual field (VF) loss. The demographic and ocular features of the VF progressing and non-progressing groups at baseline are presented in Table S9.

The patients in the progression group exhibited a statistically significant increase (P<0.001) in the mean serum levels of androstenedione compared to those in the non-progressing group (refer to Table S9). Furthermore, the multivariate Cox analysis revealed that the baseline levels of androstenedione (HR=2.71, 95% CI=1.20–6.10, P=0.017) were significantly associated with glaucoma progression, as determined by the VF loss results (Table 2). Figure 7 displays the Kaplan-Meier survival curves. The results of the survival analysis revealed a statistically significant increase in the proportion of patients with elevated androstenedione levels who experienced VF progression in PACG (log-rank test, P<0.001, Figure 7A). Comparable findings were observed in both the female (log-rank test, P=0.0042, Figure 7B) and male (log-rank test, P=0.0014, Figure 7C) subgroups.

4. Discussion

The delayed identification of PACG is a notable contributor to patients' impaired vision and irreversible blindness. Regrettably, existing medical protocols do not advocate for the use of blood-based biomarkers to diagnose and prognosticate PACG. Consequently, it is imperative to develop novel, uncomplicated, and practicable approaches to improve the early detection of PACG and its predictive

accuracy. To address the significant challenge at hand, the present study conducted a cross-sectional and prospective cohort investigation utilizing high-throughput, widely-targeted metabolomics and targeted chemiluminescence immunoassay on blood samples obtained from a substantial number of patients diagnosed with PACG and healthy individuals. The findings of this study reveal, for the first time, that androstenedione exhibits a reasonable level of precision (AUC, 0.85-1.0) in distinguishing between PACG and control groups in blood samples. Additionally, the baseline levels of androstenedione may serve as a valuable predictor of glaucomatous visual field progression.

Some metabolites have been proposed to have a potential role in discriminating PACG from normal, but validation studies in larger cohorts still need to be completed. Rong et al. [14] conducted a case-control (PACG=38, normal=48) study using gas chromatography-mass spectrometry and reported that palmitoleic acid, linoleic acid, γ-linolenic acid, and arachidonic acid were identified as essential metabolites associated with PACG, but diagnostic accuracy is unknown. In our study, these metabolites were also detected, but diagnosis accuracy (AUC<0.7) was limited. Qin et al.[24] measured plasma twenty-two free fatty acids (FFA) and six lipid classes using metabolomics analysis, shown that docosahexaenoic acid (DHA) and total saturated fatty acids may be screening indices (AUC, 0.82-0.85) for PACG patients but lack validation set to confirm the results. DHA (AUC, 0.74-0.85), FFA (22:6) (AUC, 0.74-0.85), and FFA (18:4) (AUC, 0.79-1.0) was also shown a diagnose value for PACG patients in the discovery set of our study (Figure 3A), but the robustness and diagnose accuracy was weaker than androstenedione (AUC, 0.85-1.0) (Table S10). The contribution of previous metabolites to PACG diagnosis was small, which prompted us to conduct a trial designed to develop biomarkers.

In this study, androstenedione levels achieved better diagnostic efficiency and robust calibration across the discovery and validation sets. The transformation of normal subjects into PACG is a chronic stepwise process. Given this, screening healthy individuals and those with a family history of the disease is vital. Another important finding of this research was that the level of serum androstenedione retained its diagnostic efficiency for distinguishing the severity of PACG. Furthermore, serum androstenedione levels incrementally increased from mild to moderate to severe PACG, suggesting that serum androstenedione levels may accurately reflect the progression/severity of PACG. Furthermore, androstenedione levels at baseline were a new biomarker for predicting glaucomatous VF progression. Hence, serum androstenedione levels may provide a new biomarker for early detection

436 and monitoring/predicting PACG severity/progression.

437 In the supplemental phase, we asked whether the serum levels of androstenedione were significantly
438 corrected with aqueous humor levels of androstenedione from the same PACG patients, which is an
439 important criterion for application as a routine clinical biomarker and to explore the biological function
440 in PACG. Fortunately, the levels of aqueous humor androstenedione were positively corrected (r=0.82,
441 P=0.038) with serum levels. Meanwhile, the levels of aqueous humor androstenedione incrementally
442 increased from mild-moderate to severe PACG. Furthermore, the levels of aqueous humor
443 androstenedione remained higher in PACG than in cataracts. Together, these results confirm that
444 androstenedione can serve as a novel biomarker for early detection and monitoring of the
445 progression/severity of PACG.

446 In clinical practice, oral topical glaucoma medications and laser peripheral iridectomy were the
447 primary therapies used to treat PACG. However, the effects of these therapies are mainly estimated by
448 measurement of intraocular pressure and optical coherence tomography. Thus, we have wondered
449 whether, by dynamic detection, serum androstenedione levels could reflect the therapeutic effect of
450 these therapies. In the supplemental phase (fourth phase), in a small cohort of 9 PACG patients treated
451 with laser peripheral iridectomy or oral topical glaucoma medications, which showed a better
452 prognosis, 7 of 9 exhibited decreased levels of serum androstenedione. These results shed new light
453 on the monitor the effect of therapy; however, these should be verified in a larger cohort.

454 The main strength of our study is its robustness. We conducted a 5-phase study (discovery set
455 [discovery set 1, the discovery set 2], validation phase 1, validation phase 2, supplemental phase, and
456 cohort phase). We used large and well-characterized patients with adequate controls to confirm the
457 results. Widely-targeted metabolomics and target chemiluminescence immunoassay methods provide
458 high reliability of the metabolite. Androstenedione achieved better diagnostic accuracy across the
459 discovery and validation sets, with AUC varying between 0.85 and 1.0. Interestingly, baseline
460 androstenedione levels can predict glaucoma progression via VF loss results. Of note, the clinical
461 practice of androstenedione in patients with PACG was analyzed by supplemental phase.

462 The metabolites identified by this study match PACG pathophysiological concepts. Pathway
463 enrichment analysis demonstrated that these 32 significantly altered metabolites primarily belonged to
464 16 pathways (Figure S13, Figure S14A). Among the top altered pathways, steroid hormone

biosynthesis appears to be the critical node to high-match PACG pathophysiological concepts[25,26]: it connects with androstenedione. The sex hormones pathway is a vital component of steroid hormone biosynthesis (Figure S14B). Several studies have focused on the importance of 17β-estradiol in protecting the retinal ganglion cell layer and preserving visual function in clinical[27] and basic[25] research by anti-inflammatory effect[28]. Our previous studies suggested that decreased sex hormone concentrations in glaucoma lead to a hyperinflammatory state, leading to faster rates of VF damage[18,29]. Thus, we hypothesized that aromatase defects might lead to a decrease in estradiol levels and an increase in androstenedione, causing an inflammatory response and leading to retinal ganglion cell death in patient with glaucoma (Figure S14C). In addition, androstenedione converted to estrogens is catalyzed by the aromatase (Figure S14D). Furthermore, some of the metabolites might also be linked to PACG physiological processes that remain unclear, and future research in this field is needed.

Furthermore, other studies have also found significant correlations between androstenedione and other diseases. For example, Javier et al.[30] found that androstenedione can predict the progression of Frailty Syndrome in patients with localized breast cancer treated with aromatase inhibitors. Adriaansen et al.[31] reported that diurnal salivary androstenedione levels in healthy volunteers for monitoring treatment efficacy of patients with congenital adrenal hyperplasia.

As far as our understanding goes, this is the initial investigation to methodically outline blood metabolites and scrutinize the diagnostic efficacy of a potential biomarker for PACG. Nevertheless, our study is not without its limitations: (1) The supplementary phase of our study was conducted with a restricted number of patients and healthy controls. Therefore, further investigations with larger sample sizes are necessary to confirm the diagnostic accuracy of serum androstenedione for the detection of primary angle-closure glaucoma (PACG). (2) Our study cohort exhibited uniform genetic and environmental traits, which may restrict the generalizability of our findings to populations with diverse ethnic or racial backgrounds. (3) Despite the matching of PACG patients and controls for age, gender, BMI, hypercholesterolemia, hypertension, diabetes, smoking, and drinking, it is possible that unidentified residual confounding factors could impact the observed metabolomic disparities. (4) Throughout the duration of the follow-up period, the majority of individuals received pharmacological treatment, and the study's follow-up period was limited to a mere two years. Consequently, the outcomes may have been impacted by either behavioral adjustments prompted by patients' cognizance

of their medical condition or by any form of therapeutic intervention. (5) Despite our examination of the impact of hormone intake (including estrogen, progestagen, and anti-androgen), the potential influence of reproductive aging cannot be entirely dismissed.

5. Conclusions

In conclusion, androstenedione has been identified and validated through the use of widely-targeted LC-MS or targeted chemiluminescence immunoassay, demonstrating its ability to effectively differentiate between healthy individuals and those with PACG. Additionally, baseline androstenedione levels may serve as a valuable predictor of glaucomatous VF progression. However, further clinical and basic studies are required to confirm the clinical utility of serum androstenedione for early-stage PACG diagnosis, as well as its potential for monitoring/predicting VF progression and elucidating the underlying mechanisms linking androstenedione to PACG.

Declarations

Ethics approval and consent to participate: This study was approved by the Ethics Committee of Eye and ENT Hospital of Fudan University (EENT-2015011) and was conducted under the Declaration of Helsinki. All participants provided written informed consent prior to their participation.

Consent for publication: Not applicable.

Availability of data and materials: The datasets used and/or analyzed during the current study are available from the corresponding author on reasonable request.

Competing interests: No conflicting relationship exists for any author.

Funding: This work was supported by Youth Medical Talents – Clinical Laboratory Practitioner Program (2022-65), the Excellent Physician – Excellent Clinical Researcher Plan (SYA202004). The sponsor or funding organization had no role in the design or conduct of this research.

Authors' contributions: Shengjie Li, and Wenjun Cao contributed to the study conception and design, data analysis, interpretation of the data, and drafting the manuscript. Yichao Qiu, Jun Ren, Zhendong Jiang, Yingzhu Li, Yunxiao Song, and Mingxi Shao contributed to the interpretation of the data and critical revision of the manuscript. Shengjie Li, Yichao Qiu, Jun Ren, Yingzhu Li, Yunxiao Song, Xinghuai Sun, and Mingxi Shao contributed to the collection of the data. All authors read and approved the final manuscript.

Acknowledgements: Not applicable.

Reference

1. Jonas, J. B. *et al.* Glaucoma. *Lancet* **390**, 2183–2193 (2017).
2. Liu, Y. *et al.* Glaucoma in rural China (the Rural Epidemiology for Glaucoma in China (REG-China)): a national cross-sectional study. *Br J Ophthalmol* bjophthalmol-2021-320754 (2022) doi:10.1136/bjo-2021-320754.
3. Stein, J. D. *et al.* Differences in rates of glaucoma among Asian Americans and other racial groups, and among various Asian ethnic groups. *Ophthalmology* **118**, 1031–1037 (2011).
4. Tham, Y.-C. *et al.* Global prevalence of glaucoma and projections of glaucoma burden through 2040: a systematic review and meta-analysis. *Ophthalmology* **121**, 2081–2090 (2014).
5. Song, W. *et al.* Prevalence of glaucoma in a rural northern china adult population: a population-based survey in kailu county, inner mongolia. *Ophthalmology* **118**, 1982–1988 (2011).
6. Stein, J. D., Khawaja, A. P. & Weizer, J. S. Glaucoma in Adults-Screening, Diagnosis, and Management: A Review. *JAMA* **325**, 164–174 (2021).
7. He, M. *et al.* Laser peripheral iridotomy for the prevention of angle closure: a single-centre, randomised controlled trial. *Lancet* **393**, 1609–1618 (2019).
8. Sun, X. *et al.* Primary angle closure glaucoma: What we know and what we don't know. *Prog Retin Eye Res* **57**, 26–45 (2017).
9. J, Y. *et al.* Decreased cerebrospinal fluid kynurenic acid in epileptic spasms: A biomarker of response to corticosteroids. *EBioMedicine* **84**, (2022).
10. Guijas, C., Montenegro-Burke, J. R., Warth, B., Spilker, M. E. & Siuzdak, G. Metabolomics

547 activity screening for identifying metabolites that modulate phenotype. *Nat Biotechnol* **36**, 316–
548 320 (2018).
549 11. Hysi, P. G. *et al.* Ascorbic acid metabolites are involved in intraocular pressure control in the
550 general population. *Redox Biol* **20**, 349–353 (2019).
551 12. Wang, Y., Hou, X.-W., Liang, G. & Pan, C.-W. Metabolomics in Glaucoma: A Systematic Review.
552 *Invest Ophthalmol Vis Sci* **62**, 9 (2021).
553 13. Tang, Y. *et al.* Metabolomic Profiling of Aqueous Humor and Plasma in Primary Open Angle
554 Glaucoma Patients Points Towards Novel Diagnostic and Therapeutic Strategy. *Front Pharmacol*
555 **12**, 621146 (2021).
556 14. Rong, S. *et al.* Long-chain unsaturated fatty acids as possible important metabolites for primary
557 angle-closure glaucoma based on targeted metabolomic analysis. *Biomed Chromatogr* **31**, (2017).
558 15. Kang, J. H. *et al.* Prediagnostic Plasma Metabolomics and the Risk of Exfoliation Glaucoma.
559 *Invest Ophthalmol Vis Sci* **63**, 15 (2022).
560 16. Li, S. *et al.* Serum complement component 3, complement component 4 and complement
561 component 1q levels predict progressive visual field loss in older women with primary angle
562 closure glaucoma. *Br J Ophthalmol* bjophthalmol-2021-320541 (2022) doi:10.1136/bjophthalmol-
563 2021-320541.
564 17. Li, S. *et al.* Association of systemic inflammation indices with visual field loss progression in
565 patients with primary angle-closure glaucoma: potential biomarkers for 3P medical approaches.
566 *EPMA J* **12**, 659–675 (2021).
567 18. Li, S. *et al.* Association Between 17-β-Estradiol and Interleukin-8 and Visual Field Progression in
568 Postmenopausal Women with Primary Angle Closure Glaucoma. *Am J Ophthalmol* **217**, 55–67

569 (2020).

570 19. Chen, Y. *et al.* Lack of Association of rs1192415 in TGFBR3-CDC7 With Visual Field
571 Progression: A Cohort Study in Chinese Open Angle Glaucoma Patients. *Front Genet* **9**, 488
572 (2018).

573 20. Naghizadeh, F. & Holló, G. Detection of early glaucomatous progression with octopus cluster
574 trend analysis. *J Glaucoma* **23**, 269–275 (2014).

575 21. Gong, L. *et al.* All-In-One Biomimetic Nanoplatform Based on Hollow Polydopamine
576 Nanoparticles for Synergistically Enhanced Radiotherapy of Colon Cancer. *Small* **18**, e2107656
577 (2022).

578 22. Obuchowski, N. A. & Zhou, X.-H. Prospective studies of diagnostic test accuracy when disease
579 prevalence is low. *Biostatistics* **3**, 477–492 (2002).

580 23. Li, J. & Fine, J. On sample size for sensitivity and specificity in prospective diagnostic accuracy
581 studies. *Stat Med* **23**, 2537–2550 (2004).

582 24. Qin, Y. *et al.* Association between plasma free fatty acid levels and primary angle-closure
583 glaucoma based on a mass spectrometry metabolomics analysis. *Acta Ophthalmol* **100**, e204–e212
584 (2022).

585 25. Prokai-Tatrai, K. *et al.* 17β-estradiol eye drops protect the retinal ganglion cell layer and preserve
586 visual function in an in vivo model of glaucoma. *Mol Pharm* **10**, 3253–3261 (2013).

587 26. Madjedi, K. M. *et al.* The Association of Female Reproductive Factors with Glaucoma and Related
588 Traits: A Systematic Review. *Ophthalmol Glaucoma* S2589-4196(22)00096–5 (2022)
589 doi:10.1016/j.ogla.2022.06.003.

590 27. Vajaranant, T. S. *et al.* Racial Differences in the Effects of Hormone Therapy on Incident Open-

Angle Glaucoma in a Randomized Trial. *Am J Ophthalmol* **195**, 110–120 (2018).

28. Engler-Chiurazzi, E. B., Brown, C. M., Povroznik, J. M. & Simpkins, J. W. Estrogens as neuroprotectants: Estrogenic actions in the context of cognitive aging and brain injury. *Prog Neurobiol* **157**, 188–211 (2017).
29. Qiu, Y. *et al.* Association Between Sex Hormones and Visual Field Progression in Women With Primary Open Angle Glaucoma: A Cross-Sectional and Prospective Cohort Study. *Front Aging Neurosci* **13**, 756186 (2021).
30. García-Sánchez, J., Mafla-España, M. A., Torregrosa, M. D. & Cauli, O. Androstenedione and Follicle-Stimulating Hormone Concentration Predict the Progression of Frailty Syndrome at One Year Follow-Up in Patients with Localized Breast Cancer Treated with Aromatase Inhibitors. *Biomedicines* **10**, 1634 (2022).
31. Adriaansen, B. P. H. *et al.* Diurnal salivary androstenedione and 17-hydroxyprogesterone levels in healthy volunteers for monitoring treatment efficacy of patients with congenital adrenal hyperplasia. *Clin Endocrinol (Oxf)* **97**, 36–42 (2022).

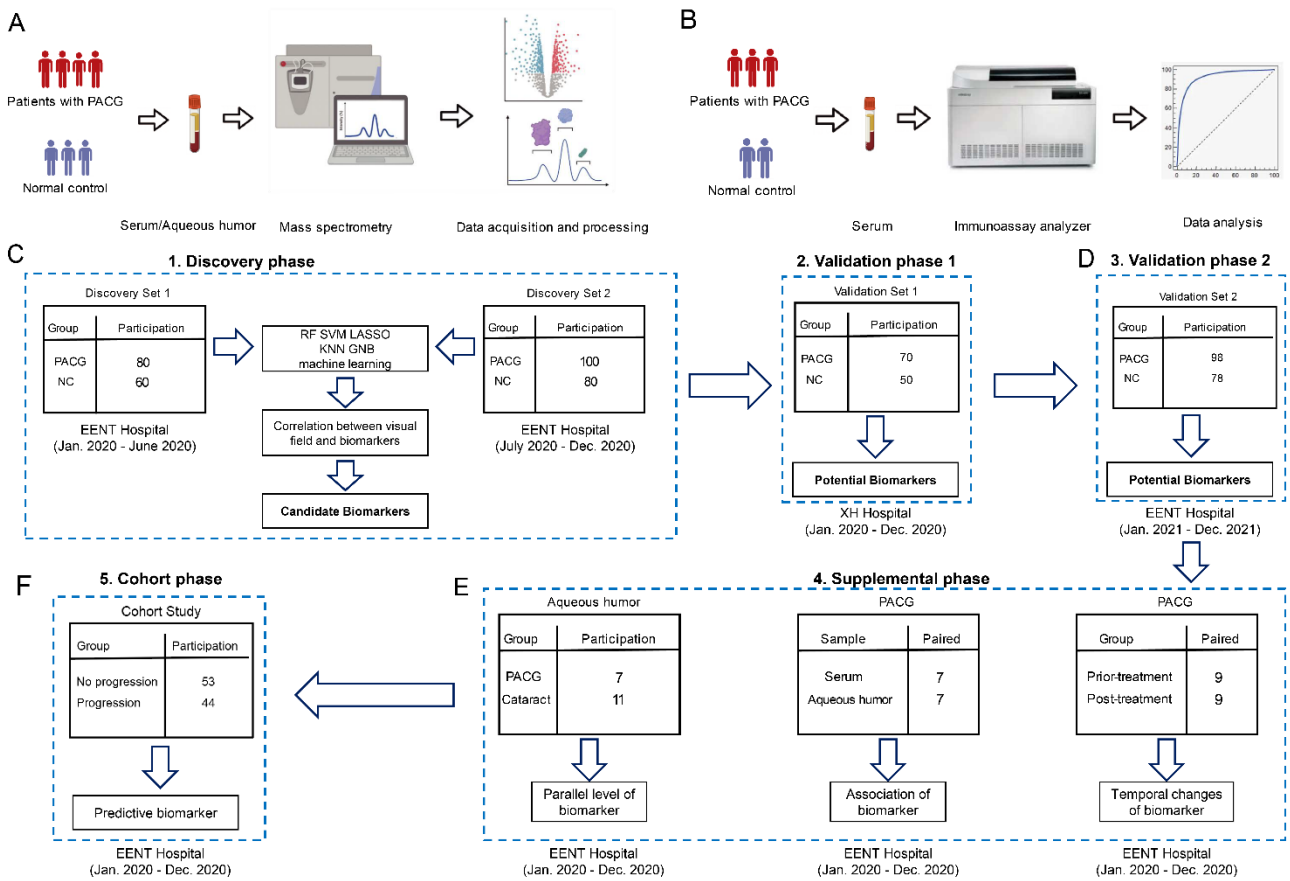

Figure 1. Study design and workflow. A 5-phase study (discovery phase [discovery set 1, the discovery set 2], validation phase 1, validation phase 2, supplemental phase, and cohort phase) design. A: The workflow of the discovery phase, validation phase 1, supplemental phase, and cohort phase were analyzed by liquid chromatography-mass spectrometry (LC-MS) for untargeted metabolomics. B: The workflow of validation phase 2 was analyzed chemiluminescence immunoassay for targeted detection. C: A total of 440 patients and controls were recruited and assigned to discovery set 1 (n = 140), the discovery set 2 (n = 180), and validation set 1 (n = 120). The biomarker signature was identified on the metabolomic data from the discovery phase, comparing primary angle closure glaucoma (PACG) with control patients. These data were used as a discovery set for the algorithm. D: Validation phase 2 (n = 176) was included as the second validation cohort. E: Three measurements were performed in the supplemental phase. F: Cohort phase were performed to validate the predictive value of biomarker (n = 97).

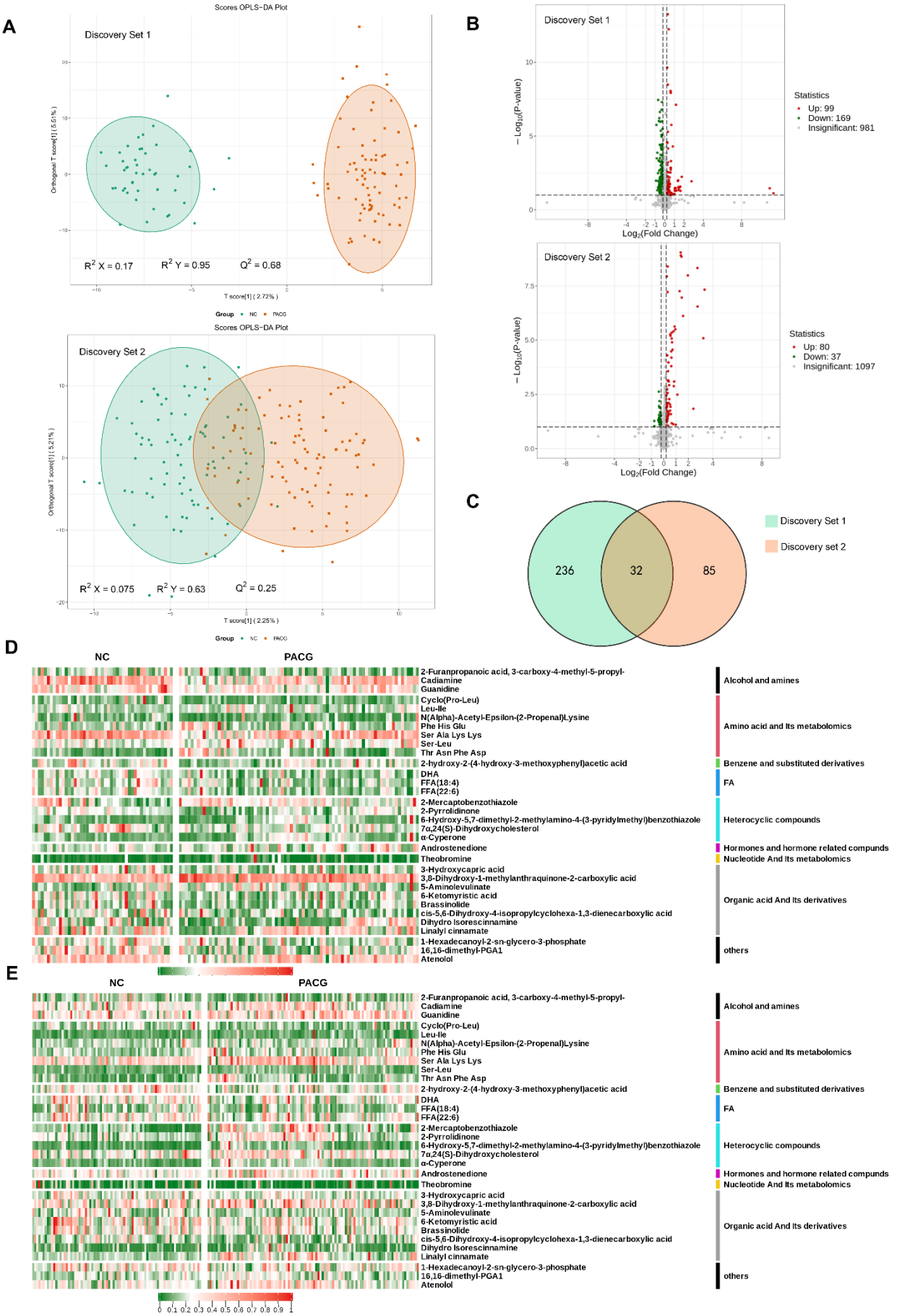
A
Scores OPLS-DA Plot
Discovery Set 1
R2 X = 0.17
R2 Y = 0.95
Q2 = 0.68
Group NC PACG
Scores OPLS-DA Plot
Discovery Set 2
R2 X = 0.075
R2 Y = 0.63
Q2 = 0.25
Group NC PACG
B
Discovery Set 1
Statistics
Up: 99
Down: 169
Insignificant: 981
Discovery Set 2
Statistics
Up: 80
Down: 37
Insignificant: 1097
C
Discovery Set 1
Discovery set 2
236
32
85
D
NC
PACG
2-Furanpropanoic acid, 3-carboxy-4-methyl-5-propyl-
Cadiamine
Guanidine
Cyclo(Pro-Leu)
Leu-Ile
N(Alpha)-Acetyl-Epsilon-(2-Propenal)Lysine
Phe His Glu
Ser Ala Lys Lys
Ser-Leu
Thr Asn Phe Asp
2-hydroxy-2-(4-hydroxy-3-methoxyphenyl)acetic acid
DHA
FFA(18:4)
FFA(22:6)
2-Mercaptobenzothiazole
2-Pyrrolidinone
6-Hydroxy-5,7-dimethyl-2-methylamino-4-(3-pyridylmethyl)benzothiazole
7α,24(S)-Dihydroxycholesterol
α-Cyperone
Androstenedione
Theobromine
3-Hydroxycapric acid
3,8-Dihydroxy-1-methylanthraquinone-2-carboxylic acid
5-Aminolevulinate
6-Ketomyristic acid
Brassinolide
cis-5,6-Dihydroxy-4-isopropylcyclohexa-1,3-dienecarboxylic acid
Dihydro Isorescinnamine
Linalyl cinnamate
1-Hexadecanoyl-2-sn-glycero-3-phosphate
16,16-dimethyl-PGA1
Atenolol
Alcohol and amines
Amino acid and Its metabolomics
Benzene and substituted derivatives
FA
Heterocyclic compounds
Hormones and hormone related compunds
Nucleotide And Its metabolomics
Organic acid And Its derivatives
others
E
NC
PACG
0 0.1 0.2 0.3 0.4 0.5 0.6 0.7 0.8 0.9 1

619

Figure 2. Metabolic profiles discriminate participants with primary angle closure glaucoma (PACG) from normal controls (NC). A: Orthogonal projection to latent structure-discriminant analysis (OPLS-DA) score plot of the comparison between the PACG and NC groups in the discovery phase (discovery set 1 and discovery set 2). Samples in the encircled areas are within the 95% confidence interval. B: Volcano plot of differential metabolites. Metabolites with a fold change of <0.85 and a false discovery rate (FDR) of <0.1 were considered significantly down-regulated. Metabolites with a fold change of >1.15 and an FDR of <0.1 were considered significantly up-regulated. Changes in other metabolites were not significant (insignificant). C: Venn diagram displaying the 32 differential metabolites that were altered as biomarker candidates from the two comparisons in the discovery phase. D: Heatmap of differential metabolites in the discovery set 1 (Data were normalized to min-max). E: Heatmap of differential metabolites in the discovery set 2 (Data were normalized to min-max). FA: fatty acid.

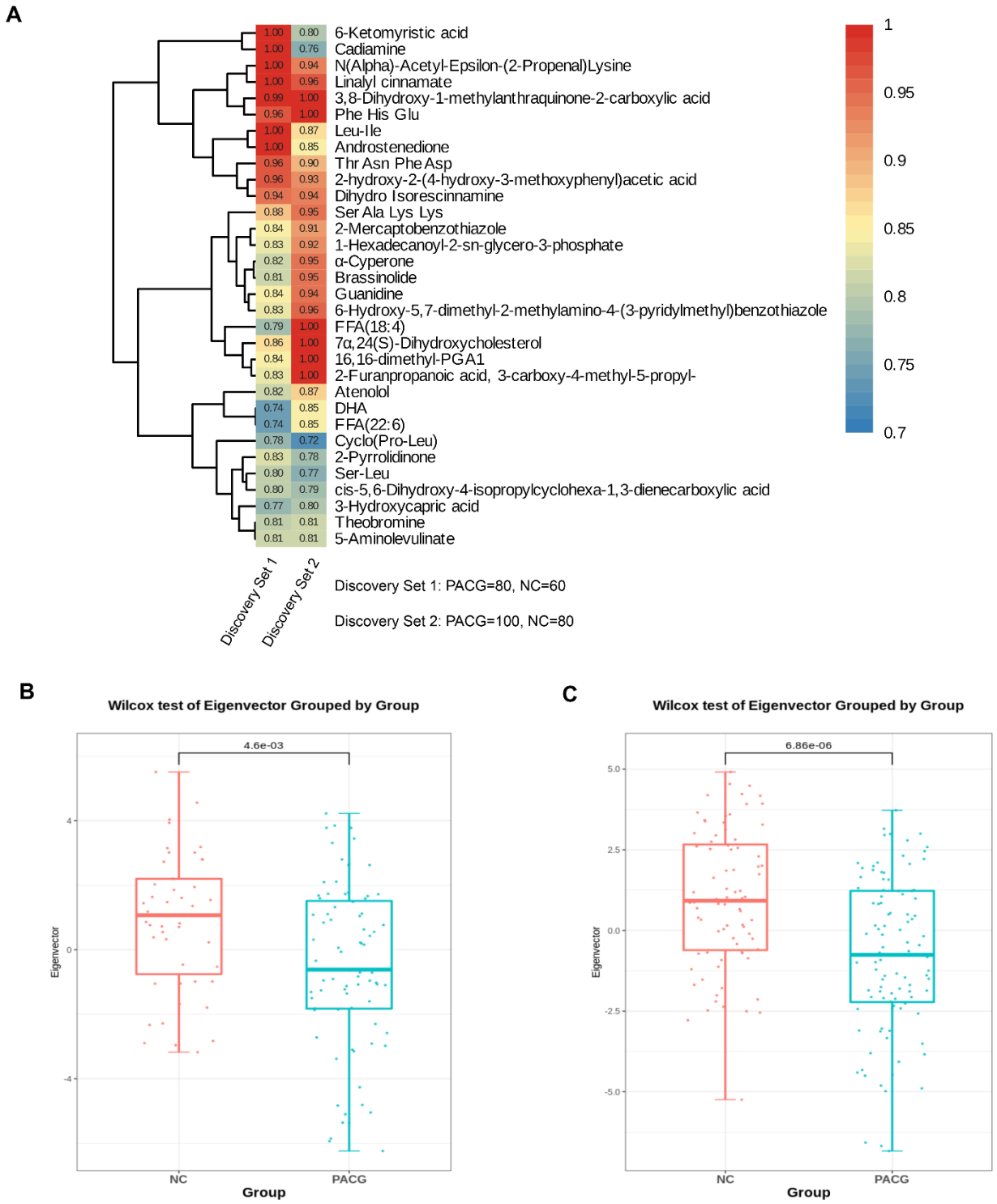

Figure 3. Identification of a unique PACG-associated blood metabolite fingerprint and its behavior in the discovery phase. A: Heatmap of the area under the receiver-operating-characteristic curve assessing the discriminating accuracy of each of the 32 metabolites in differentiating PACG from normal control

635 in the discovery set 1 and discovery set 2. B: The eigenmetabolite of the 32-metabolite cluster between
636 primary angle closure glaucoma (PACG) and control patients in the discovery set 1. C: The
637 eigenmetabolite of the 32-metabolite cluster between primary angle closure glaucoma (PACG) and
638 control patients in the discovery set 2. Wilcox test was used.

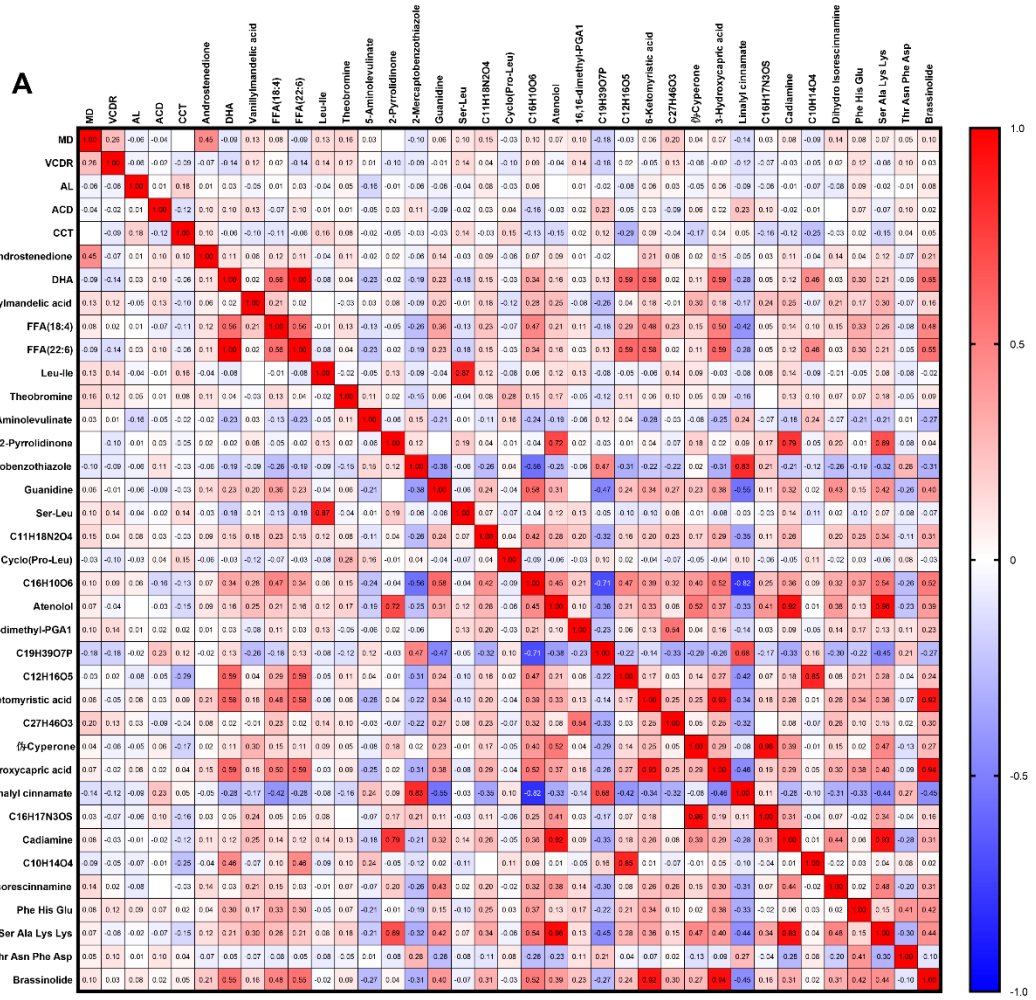
A
MD
VCDR
AL
ACD
CCT
Androstenedione
DHA
Vanillylmandelic acid
FFA(18:4)
FFA(22:6)
Leu-Ile
Theobromine
5-Aminolevulinate
2-Pyrrolidinone
2-Mercaptobenzothiazole
Guanidine
Ser-Leu
C11H18N2O4
Cyclo(Pro-Leu)
C16H10O6
Atenolol
16,16-dimethyl-PGA1
C19H39O7P
C12H16O5
6-Ketomyristic acid
C27H46O3
仿Cyperone
3-Hydroxycapric acid
Linalyl cinnamate
C16H17N3OS
Cadiamine
C10H14O4
Dihydro Isorescinnamine
Phe His Glu
Ser Ala Lys Lys
Thr Asn Phe Asp
Brassinolide
1.0
0.5
0
-0.5
-1.0

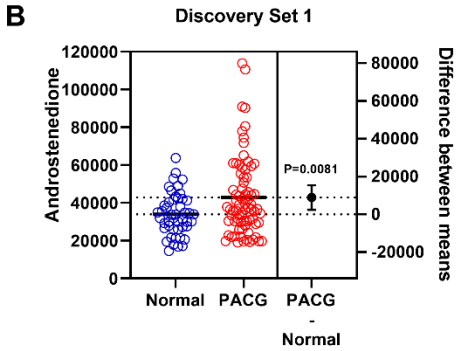
B
Discovery Set 1
Androstenedione
Difference between means
P=0.0081
Normal
PACG
PACG - Normal

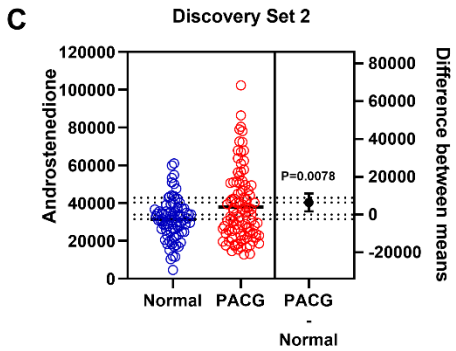
C
Discovery Set 2
Androstenedione
Difference between means
P=0.0078
Normal
PACG
PACG - Normal

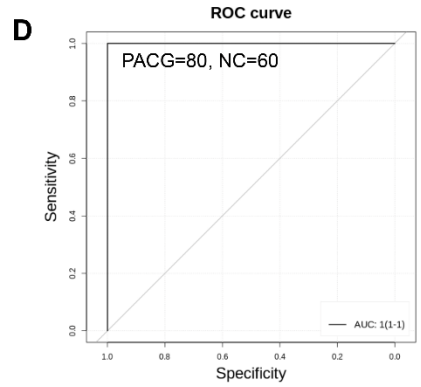
D
ROC curve
PACG=80, NC=60
Sensitivity
Specificity
AUC: 1(1-1)

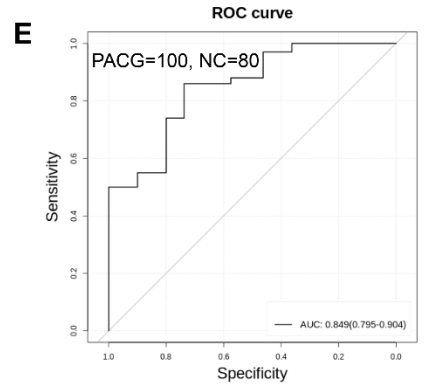
E
ROC curve
PACG=100, NC=80
Sensitivity
Specificity
AUC: 0.849(0.795-0.904)

639

640 **Figure 4.** Biomarker discovery discriminates primary angle closure glaucoma (PACG) from normal in
641 the discovery phase. A: A heatmap of correlation analysis between ocular clinical characteristics and
642 32 potential biomarkers in the discovery phase in PACG subjects. B: The serum level of
643 androstenedione between PACG and normal group in the discovery set 1 (Unit for y-axis is peak areas).
644 C: The serum level of androstenedione between PACG and normal group in the discovery set 2 (Unit
645 for y-axis is peak areas). D: Receiver operating characteristic curves of androstenedione to
646 discriminate PACG from normal in the discovery set 1. E: Receiver operating characteristic curves of
647 androstenedione to discriminate PACG from normal in the discovery set 2. Independent student's t-test
648 was used.

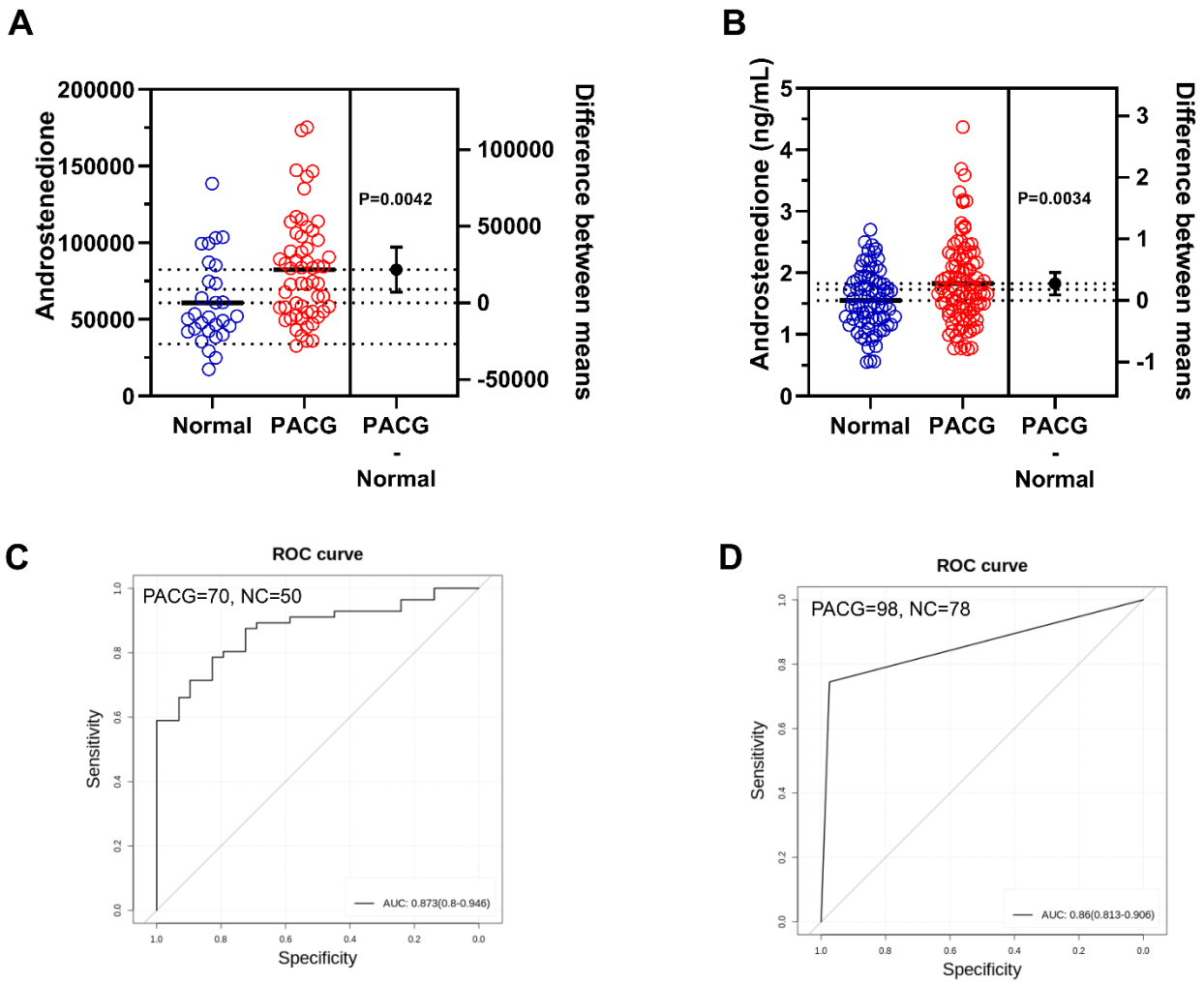

649

650 **Figure 5.** Biomarker validation in two independent validation phases to discriminate primary angle
651 closure glaucoma (PACG) from normal. A: The serum level of androstenedione between PACG and
652 normal group in validation phase 1 (Unit for y-axis is peak areas). B: The serum level of

androstenedione between PACG and normal group in validation phase 2 (Unit for y-axis is peak areas). C: Receiver operating characteristic curves of androstenedione to discriminate PACG from normal in validation phase 1. D: Receiver operating characteristic curves of androstenedione to discriminate PACG from normal in validation phase 2. Independent student's t-test was used.

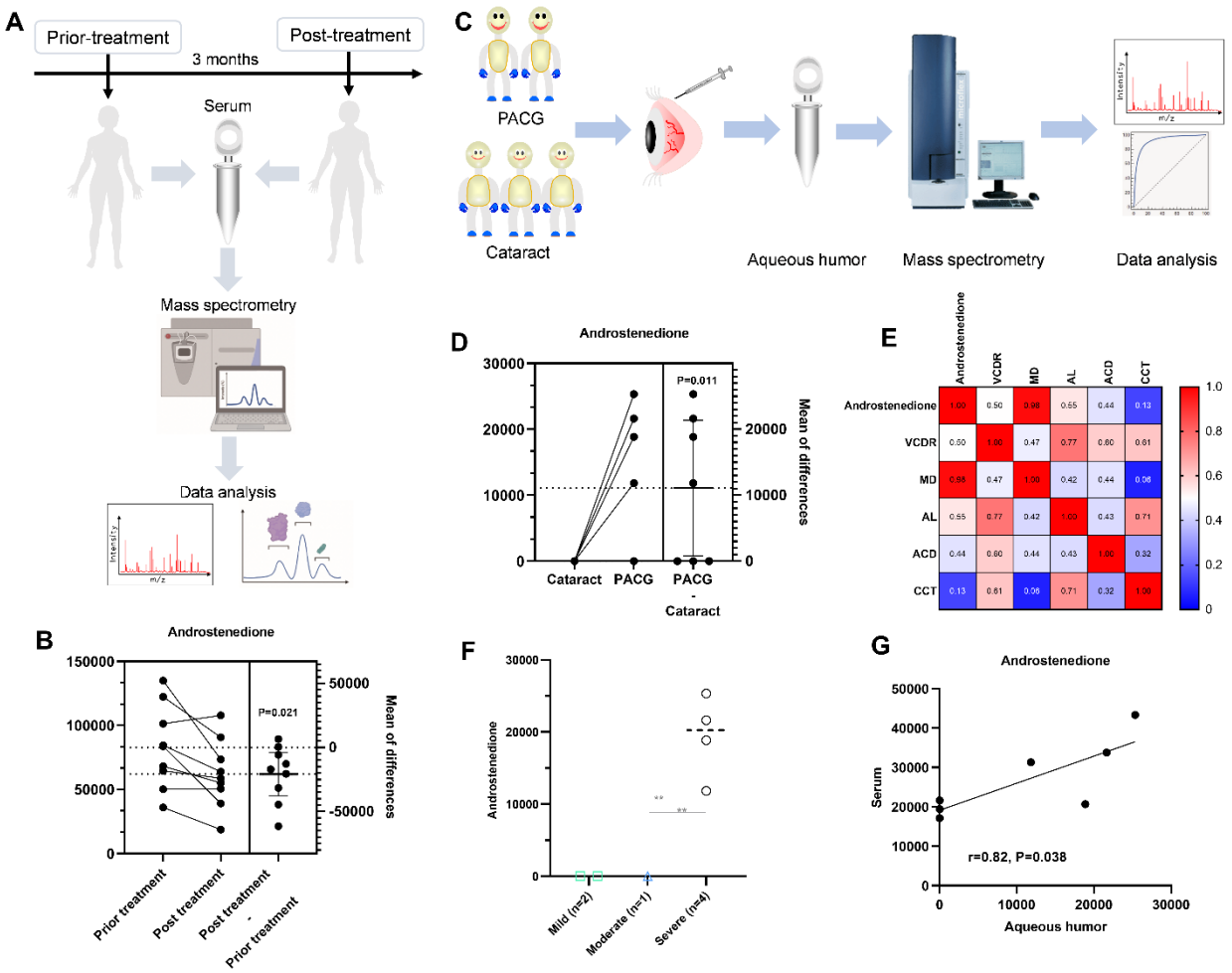

Figure 6. Specificity of circulating androstenedione in patients with primary angle closure glaucoma (PACG) in supplemental phase. A: Sampling scheme and workflow to investigate the temporal changes in androstenedione levels. B: Differential level of serum androstenedione between patients with PACG before and three months after treatment (Unit for y-axis is peak areas). C: Sampling scheme and workflow to determine whether aqueous humor levels of androstenedione were high in patients with PACG. D: The aqueous humor level of androstenedione between PACG and cataract (Unit for y-axis is peak areas). E: Heatmap of correlation analysis between ocular clinical characteristics and aqueous humor level of androstenedione. F: Comparison means aqueous humor levels of androstenedione between mild, moderate, and severe PACG (Unit for y-axis is peak areas). G: 7 paired serum-aqueous

humor samples from the same PACG patients were included (Unit for y and x-axis is peak areas). A significant correlation between serum and aqueous humor levels of androstenedione was observed. Kruskal-Wallis test and one-way ANOVA was used. *P<0.05; **: P<0.001.

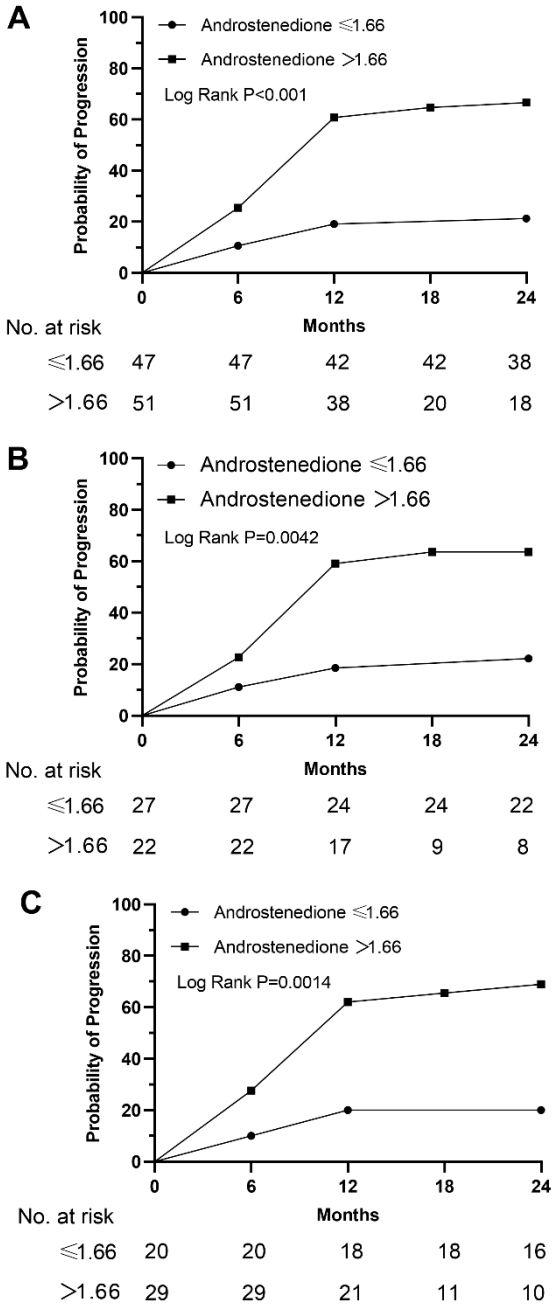

Figure 7. Kaplan-Meier curves stratified by the men value in terms of androstenedione. A: male+female; B: Female; C: Male. We categorized study participants into 2 groups based on their mean levels of androstenedione.

Table 1. The clinical and demographic characteristics of all subjects in the discovery and validation phases

	Normal (n=268)	PACG (n=348)	t/χ^2	p
Discovery phase				
Discovery set 1				
Number (n)	60	80		
Age (Years)	58.75±8.63	61.00±8.67	1.52	0.13
Sex（Male，%）	24（40.0）	31（38.8）	0.02	0.88
BMI (Kg/m^2)	24.04±5.27	23.36±2.44	0.99	0.33
Hypercholesterolemia（Yes，%）	6 (10)	9 (11.3)	0.06	0.81
Hypertension (Yes，%)	16（26.7）	18（22.8）	0.32	0.60
Diabetes (Yes，%)	1（1.7）	8（10.1）	3.96	0.10
Smoking (Yes，%)	5（8.3）	11（13.9）	0.99	0.42
Drinking (Yes，%)	7（11.7）	8（10.1）	0.1	0.76
Duration (Months)		10.45±12.43		
IOP（mmHg)	12.22±4.50	27.78±11.20	10.17	<0.001
VCDR	0.25±0.18	0.64±0.23	10.87	<0.001
AL (mm)		22.48±1.14		
ACD (mm)		1.86±0.55		
CCT (um)		534.04±41.26		
MS (dB)		12.46±8.75		
MD (dB)		14.67±8.94		
Discovery set 2				
Number (n)	80	100		
Age (Years)	62.54±6.74	63.14±9.04	0.49	0.62
Sex（Male，%）	35 (43.8)	33 (33.0)	2.19	0.14
BMI (Kg/m^2)	23.68±2.81	23.32±3.15	1.36	0.18
Hypercholesterolemia (Yes，%)	12 (15)	13 (13)	0.15	0.70
Hypertension (Yes，%)	26 (32.5)	33 (33.0)	0.01	0.94
Diabetes (Yes，%)	7 (8.8)	9 (9.0)	0.003	0.95
Smoking (Yes，%)	11 (13.8)	15 (15.0)	0.06	0.81
Drinking (Yes，%)	19 (23.8)	22 (22.0)	0.08	0.78

Duration (Months)		8.46±9.69		
IOP (mmHg)	11.45±5.21	25.80±12.55	8.329	<0.001
VCDR	0.27±0.14	0.61±0.22	10.48	<0.001
AL (mm)		22.43±0.75		
ACD (mm)		2.05±0.77		
CCT (um)		547.43±43.04		
MS (dB)		12.34±8.55		
MD (dB)		14.50±8.95		
Validation phase 1				
Number (n)	50	70		
Age (Years)	57.47±8.17	60.34±10.11	1.66	0.10
Sex（Male，%）	18 (36.0)	24 (34.3)	0.04	0.85
BMI (Kg/m^2)	23.08±1.99	24.45±3.72	1.31	0.19
Hypercholesterolemia (Yes，%)	4 (8)	8 (11.4)	0.38	0.54
Hypertension (Yes，%)	17 (34.0)	21 (30.0)	0.22	0.64
Diabetes (Yes，%)	5 (10.0)	7 (10.0)	0.0	1.0
Smoking (Yes，%)	6 (12.0)	10 (14.3)	0.13	0.72
Drinking (Yes，%)	10 (20.0)	15 (21.4)	0.04	0.85
Duration (Months)		11.09±13.82		
IOP (mmHg)	12.90±4.11	28.46±9.80	11.55	<0.001
VCDR	0.24±0.17	0.60±0.21	10.87	<0.001
AL (mm)		22.44±0.83		
ACD (mm)		1.86±0.37		
CCT (um)		539.09±82.70		
MS (dB)		13.78±8.58		
MD (dB)		13.96±9.29		
Validation phase 2				
Number (n)	78	98		
Age (Years)	56.55±11.53	60.26±15.41	1.77	0.08
Sex（Male，%）	29 (37.2)	48 (49.0)	2.46	0.12
BMI (Kg/m^2)	24.54±5.42	25.90±7.51	1.26	0.21
Hypercholesterolemia (Yes，%)	11 (14.1)	13 (13.3)	0.03	0.87
Hypertension (Yes，%)	19 (24.4)	31 (31.6)	0.26	0.61
Diabetes (Yes，%)	6 (7.7)	17 (17.3)	3.6	0.06

Smoking (Yes，%)	9 (11.5)	22 (22.4)	3.6	0.06
Drinking (Yes，%)	12 (15.4)	19 (19.4)	0.48	0.49
Duration (Months)		11.40±13.8		
IOP (mmHg)	13.40±5.43	29.20±11.20	10.07	<0.001
VCDR	0.30±0.19	0.68±0.23	10.41	<0.001
AL (mm)		23.20±1.72		
ACD (mm)		2.15±0.67		
CCT (um)		546.71±50.35		
MS (dB)		11.07±8.54		
MD (dB)		16.49±8.64		

BMI =body mass index; IOP = intraocular pressure, VCDR = vertical cup-to-disc ratio, AL = axial length, CCT = central corneal thickness, ACD = anterior chamber depth, MD: visual field mean deviation, MS: visual field mean sensitivity, PACG=primary angle closure glaucoma.

Table 2. Cox Proportional Hazards Regression Analysis to Assess the Value of Androstenedione Associated with Progression of PACG

	Univariate		Multivariate*	
	P	HR (95%CI)	P	HR (95%CI)
Age	**0.008**	**0.97 (0.95 to 0.99)**	0.22	0.98 (0.95 to 1.01)
Sex	0.87	0.95 (0.53 to 1.72)	0.73	1.15 (0.53 to 2.52)
IOP	0.59	1.007 (0.98 to 1.04)	0.75	0.99 (0.96 to 1.03)
VCDR	0.17	0.40 (0.11 to 1.46)	0.16	0.37 (0.092 to 1.46)
CCT	0.77	1.001 (0.10 to 1.007)	0.90	1.000 (0.99 to 1.007)
ACD	**0.03**	**1.63 (1.05 to 2.52)**	0.91	1.041 (0.51 to 2.13)
AL	**0.005**	**1.24 (1.07 to 1.44)**	0.35	1.12 (0.89 to 1.41)
MD	0.13	1.04 (0.99 to 1.08)	0.075	1.047 (0.10 to 1.10)
Androstenedione	**<0.001**	**3.73 (1.84 to 7.57)**	**0.017**	**2.71 (1.20 to 6.10)**

IOP = intraocular pressure, VCDR = vertical cup-to-disc ratio, AL = axial length, CCT = central corneal thickness, ACD = anterior chamber depth, MD = mean deviation, PACG=primary angle closure glaucoma.

*adjusted for BMI, diabetes (yes=1, no=0), hypertension (yes=1, no=0), hypercholesterolemia (yes=1, no=0), smoking (yes=1, no=0), and drinking (yes=1, no=0).